

https://doi.org/10.1070/QEL16450

Radial acceleration of ions during adiabatic expansion of a multicomponent cylindrical plasma

V.F. Kovalev, S.G. Bochkarev, V.Yu. Bychenkov

Abstract. **The methods of modern group analysis allow an analytic solution of the Cauchy problem to be constructed for the system of kinetic equations for a fully ionised electron–ion plasma, describing the acceleration of ions during the adiabatic expansion of a cylindrical plasma. Time and spatial dependences of the distribution functions of particles are obtained and their integral characteristics, such as density, average velocity, temperature, and energy spectrum, are found. The formation of the energy spectrum of accelerated ions, asymptotically repeating the spatial distribution of their density, and the cooling of electrons in the process of ion acceleration are analytically described. Particular attention is paid to the investigation of the influence of the heavy ionic component on the dynamics of the light component. The features of ion acceleration in the case of a two-temperature electron distribution function that describes the presence of hot and cold electron components are studied, which corresponds to the typical conditions of the experiment on plasma heating by intense laser radiation.**

Keywords: *ultrashort laser pulses, laser plasma, laser acceleration of ions, targets of 'nanoforest' type.*

1. Introduction

The generation of ions in a plasma produced by a high-power laser pulse is presently of interest for such applications as the development of compact radiation sources with record-high densities of secondary particle fluxes based on nuclear reactions by laser-accelerated ions [1], radiation medicine and nuclear pharmacology [2–4], radiography [5, 6], fast ignition for laser thermonuclear fusion [7, 8], etc. Numerous schemes have now been proposed for obtaining high-energy ions [9, 10] by ultra-short high-intensity lasers. Among all possible schemes for laser-driven particle acceleration, we note those corresponding to the expansion of plasma formations of cylindrical type. A natural implementation of such a scheme is the radial expansion of a heated laser-plasma channel arising in the caustic of a focused laser beam or during its self-focusing [11], and the expansion of cylindrical nanotubes irradiated with the laser radiation [12].

In addition, innovative high-average-density targets with an artificial substrate coating have been recently discussed. The structure of such targets consists of numerous nano-/microwires stretched along the normal to the surface (nano-forest targets) [13]. It has been demonstrated that under laboratory conditions, when such targets are irradiated by ultrahigh-energy density pulses, pressures exceeding 1 Gbar can be reached in the produced plasma [14]. Note that such pressures are characteristic for 'extreme' astrophysical objects. Targets of this type are expected to be effective for the laser triggering of nuclear reactions in the plasma of radially expanding numerous plasma microcylinders due to its high average density [1]. It is important to note that to produce a neutron source on the basis of such a scheme, high energies of accelerated particles will not be required if use is made of D- or DT-enriched microwires to initiate synthesis reactions. This will allow the use of relatively low-intensity laser radiation. The practical realisation of the above-mentioned problems must be preceded by a theoretical study of the radial expansion of a heated cylindrical plasma, which is the subject of this work.

Since the publication of Gurevich et al.'s paper [15] on the expansion of plasma into vacuum, the problem of ion acceleration has been considered in numerous formulations, including both different geometries (plane, cylindrical and spherical) and various physical models of plasma description (hydrodynamic and kinetic). The electrostatic acceleration of ions in a plasma under the action of laser radiation is based on the effect of particle acceleration by a charge separation field when plasma electrons 'break away' from ions as a result of laser-driven acceleration or heating. The separation of the charges can be practically complete if the electrons are removed from the plasma by the laser field and the ions are accelerated by the intrinsic Coulomb field (Coulomb explosion [16–18]), or be negligibly small (quasi-neutral [19, 20] or close-to-quasi-neutral [21]). In addition, an intermediate variant is possible between these limiting cases (see, for example, [22–24]), which causes the variability of plasma dynamics under the action of laser radiation.

The duration of a laser pulse acting on a plasma and producing an accelerating electric field is an important factor that determines the dynamics of plasma particles. For a long laser pulse, when the typical duration τ_L (subpicosecond/pico-

V.F. Kovalev Keldysh Institute of Applied Mathematics, Russian Academy of Sciences, Miusskaya pl. 4, 125047 Moscow, Russia; Centre for Fundamental and Applied Research, All-Russia Research Institute of Automatics, ul. Sushchevskaya 22, 127055 Moscow, Russia; P.N. Lebedev Physical Institute, Russian Academy of Sciences, Leninsky prosp. 53, 119991 Moscow, Russia;
S.G. Bochkarev P.N. Lebedev Physical Institute, Russian Academy of Sciences, Leninsky prosp. 53, 119991 Moscow, Russia; e-mail: bochkar@lebedev.ru;
V.Yu. Bychenkov P.N. Lebedev Physical Institute, Russian Academy of Sciences, Leninsky prosp. 53, 119991 Moscow, Russia; Centre for Fundamental and Applied Research, All-Russia Research Institute of Automatics, ul. Sushchevskaya 22, 127055 Moscow, Russia

Received 15 June 2017; revision received 11 August 2017
Kvantovaya Elektronika **47** (11) 1023–1030 (2017)
Translated by I.A. Ulitkin

second) is much longer than the ion acceleration time, an isothermal expansion regime with a specified thermal electron energy is usually considered [21, 22, 24]. In the case of a short (femtosecond) pulse, whose duration τ_L is small in comparison with the characteristic ion acceleration time, an adiabatic regime characterised by the cooling of electrons, whose thermal energy (obtained from the laser) is converted into the energy of accelerated ions, is typical for the expansion of a plasma (see, for example, [17, 20]). This case is considered in the present paper devoted to a detailed study of the adiabatic radial expansion of a cylindrical plasma in the quasi-neutral approximation, which is of interest both for interpreting recently obtained experimental results [25, 26] and for planning new experiments using artificial microwires on target surfaces. Note that for a long laser pulse, a competitive mechanism for accelerating ions under conditions of cylindrical geometry is the mechanism of ponderomotive ion acceleration. The latter is characteristic for the expansion of a laser-plasma channel [11]. The dominance of one or the other mechanism – thermal or ponderomotive – can be established by comparing the analytically obtained characteristics of accelerated particles.

In this paper we propose an analytic theory that relies on the methods of modern group analysis to find solutions to the kinetic equations for the electron and plasma ion distribution functions in the model of adiabatic expansion of a cylindrical plasma. We have shown that the renormalisation-group approach is an effective tool for the analytical solution of problems of laser-plasma acceleration of charged particles [20, 27, 28].

The work consists of four sections and an Appendix. In Section 2, the initial equations for the theoretical analysis of the process of plasma particle scattering are formulated. Using the renormalisation-group approach to these equations, invariant-group analytic solutions of the initial problem for the kinetic equations of plasma particles are constructed on the basis of a group of symmetries of special form (most of the formulas related to the finding of the group are listed in the Appendix). As an example, these solutions are analysed for the case of a plasma with initial Maxwellian velocity distribution functions (Section 3). A situation typical for the experiment is studied when there is a heavy (dominant) ionic component and an impurity light component, and the electron distribution function, apart from the main component, has a hot component. All this determines the maximum energy of the expanding impurity ions. Section 4 discusses the results obtained and summarises the paper. The Appendix contains formulas that illustrate the symmetry properties of the equations under discussion and explain how to construct an analytical solution.

2. Initial equations: electron–ion plasma

The dynamics of the adiabatic expansion of a cylindrical plasma bunch is determined by the solutions of the kinetic equations for the distribution functions of plasma particles of type α (electrons and ions). Taking into account the axial symmetry of the problem along the cylinder axis z and considering these equations in the cylindrical coordinates $\{t, r, \varphi, z, v_r^\alpha, v_\varphi^\alpha, v_z^\alpha\}$, we assume the particle distribution functions to be independent of the coordinates z and φ, and the velocity distribution along z is taken to be Maxwellian (for each group of particles) with temperatures T_α. We also assume that the electric field in the plasma is axially symmetric, having a unique nonzero component $E_r(t, r)$ along the radius r. Taking these assumptions into account, we obtain a simple equation for the velocity of the distribution function of particles of type α, integrated over the z-component, i.e., for

$$f_\perp^\alpha(t,r,v_r^\alpha,v_\varphi^\alpha) = \int_{-\infty}^{\infty} \mathrm{d}v_z^\alpha f^\alpha,$$

which we will consider as the initial one:

$$\frac{\partial f_\perp^\alpha}{\partial t} + v_r^\alpha \frac{\partial f_\perp^\alpha}{\partial r} + \frac{v_\varphi^\alpha}{r}\left(v_\varphi^\alpha \frac{\partial f_\perp^\alpha}{\partial v_r^\alpha} - v_r^\alpha \frac{\partial f_\perp^\alpha}{\partial v_\varphi^\alpha}\right) + \frac{e^\alpha}{m^\alpha} E_r \frac{\partial f_\perp^\alpha}{\partial v_r^\alpha} = 0. \quad (1)$$

Here, m^α and e^α are the mass and charge of type α particles. In this paper, the case of an electron–ion plasma with two types of ions will be analysed in detail, which corresponds to two possible values, $i = 1$ and $i = 2$. In this case, $e^e = -e$ and $e^i = Z_i e$, where Z_i is the charge number of ions; and $m^e = m$ and $m^i = M_i$.

Kinetic equations (1) should be used together with the equation that determines the quasi-neutrality condition in the plasma,

$$\sum_\alpha e^\alpha \int_{-\infty}^{\infty} \mathrm{d}v_r^\alpha \int_{-\infty}^{\infty} \mathrm{d}v_\varphi^\alpha f_\perp^\alpha = 0. \quad (2)$$

Solutions to equations of form (1), (2) with the use of the renormalisation-group approach were discussed previously in the application to the problem of adiabatic expansion of the plasma in plane [20, 27] and spherical [28] geometries. This approach relies on the idea of the renormalisation-group symmetry of the solution with the corresponding infinitesimal operator, under the action of which the solution to the unknown initial problem for $t = 0$ is transformed into a solution for $t \neq 0$. In this case, the particle distribution functions are written in terms of the invariants of the renormalisation-symmetry operator. Applied to the initial problem for equations (1), (2) with the initial conditions corresponding to the initial distribution functions of particles with homogeneous initial temperature and zero initial mean velocity, the equations for the particle distribution functions are as follows:

$$\begin{aligned} f_\perp^\alpha &= F^\alpha\left[\frac{1}{2}(i_{\alpha1}^2 + i_{\alpha2}^2 + \Omega^2 i_0^2) + \frac{e^\alpha m}{m^\alpha e}\Phi(i_0)\right], \\ E_r &= -\frac{m/e}{(1+\Omega^2 t^2)^{3/2}}\frac{\partial \Phi}{\partial i_0}, \\ i_0 &= \frac{r}{\sqrt{1+\Omega^2 t^2}},\ i_{\alpha1} = \sqrt{1+\Omega^2 t^2}\,(v_r^\alpha - u), \\ i_{\alpha2} &= \sqrt{1+\Omega^2 t^2}\, v_\varphi^\alpha,\quad \Omega^2 = \frac{c_s^2}{L^2}, \end{aligned} \quad (3)$$

where $u = \Omega^2 rt/(1+\Omega^2 t^2)$ is the local plasma flow rate; Ω is the frequency determined by the ratio of the sound velocity c_s to the characteristic initial plasma-cylinder radius L; and $c_s = \sqrt{Z_1 T_c / M_1}$ is the characteristic sound velocity determined by the ions of main type with charge Z_1 and mass M_1 and the temperature of cold electrons T_c, which is confirmed by works [22, 23]. Note that, although the found solution is suitable for

an arbitrary number of particle types, we will study below the situation when there is a basic ionic component and a small impurity, and the electron distribution function is a two-temperature one, i.e., it contains hot and cold components. The electric potential Φ introduced in (3) is renormalised, $e\Phi/m \to \Phi$, and, thus, it has the dimension of the square of the velocity. Its dependence on the invariant i_0 is found from the quasi-neutrality condition (2), which, taking (3) into account, takes the form

$$\sum_\alpha e^\alpha \int_{-\infty}^{\infty} \mathrm{d}i_{\alpha 1} \int_{-\infty}^{\infty} \mathrm{d}i_{\alpha 2} F^\alpha = 0. \tag{4}$$

In the next section, we analyse solutions (3), (4) for the case of a plasma with initial Maxwellian particle distribution functions.

3. Adiabatic expansion of the Maxwellian plasma. Integral characteristics of accelerated particles

Let us concretise solutions (3), (4) for the case of a plasma with initial Maxwellian distributions of ions of two types with charges $e^1 = Z_1 e$ and $e^2 = Z_2 e$, maximum concentrations n_{10} and n_{20}, and temperatures T_1 and T_2. The initial distribution function for electrons is taken as the sum of two Maxwellian velocity distributions with different thermal velocities, maximum concentrations n_{c0} and n_{h0}, and temperatures T_c and T_h for cold and hot electrons, respectively. Then for the functions $f_\perp^\alpha$ we obtain:

$$f_\perp^{\mathrm{c}} = \frac{n_{\mathrm{c}0}}{2\pi V_{T_{\mathrm{c}}}^2} \exp\left[-\frac{1}{2V_{T_{\mathrm{c}}}^2}\left(i_{e1}^2 + i_{e2}^2 + \rho^2\right) + \frac{\Phi(i_0)}{V_{T_{\mathrm{c}}}^2} \right],$$

$$f_\perp^{\mathrm{h}} = \frac{n_{\mathrm{h}0}}{2\pi V_{T_{\mathrm{h}}}^2} \exp\left[-\frac{1}{2V_{T_{\mathrm{h}}}^2}\left(i_{e1}^2 + i_{e2}^2 + \rho^2\right) + \frac{\Phi(i_0)}{V_{T_{\mathrm{h}}}^2} \right],$$

$$f_\perp^1 = \frac{n_{10}}{2\pi V_{T_1}^2} \exp\left[-\frac{1}{2V_{T_1}^2}\left(i_{11}^2 + i_{12}^2 + \rho^2\right) - \frac{Z_1 m}{M_1}\frac{\Phi(i_0)}{V_{T_1}^2} \right], \tag{5}$$

$$f_\perp^2 = \frac{n_{20}}{2\pi V_{T_2}^2} \exp\left[-\frac{1}{2V_{T_2}^2}\left(i_{21}^2 + i_{22}^2 + \rho^2\right) - \frac{Z_2 m}{M_2}\frac{\Phi(i_0)}{V_{T_2}^2} \right],$$

where $\rho = \Omega i_0$; $f_\perp^{\mathrm{e}} = f_\perp^{\mathrm{h}} + f_\perp^{\mathrm{c}}$ is the electron distribution function. Here, the potential $\Phi(i_0)$ is determined through the plasma parameters by the solution of the transcendental equation:

$$n_{\mathrm{c}0} \exp\left(-\frac{\rho^2}{2V_{T_{\mathrm{c}}}^2} + \frac{\Phi}{V_{T_{\mathrm{c}}}^2} \right) + n_{\mathrm{h}0} \exp\left(-\frac{\rho^2}{2V_{T_{\mathrm{h}}}^2} + \frac{\Phi}{V_{T_{\mathrm{h}}}^2} \right)$$
$$= Z_1 n_{10} \exp\left(-\frac{\rho^2}{2V_{T_1}^2} - \frac{Z_1 m}{M_1}\frac{\Phi}{V_{T_1}^2} \right)$$
$$+ Z_2 n_{20} \exp\left(-\frac{\rho^2}{2V_{T_2}^2} - \frac{Z_2 m}{M_2}\frac{\Phi}{V_{T_2}^2} \right). \tag{6}$$

Without loss of generality, we can choose $\Phi(0) = 0$ and, thus, obtain the relation between the maximum concentrations:

$$\sum_i Z_i n_{i0} = n_{\mathrm{c}0} + n_{\mathrm{h}0} = n_{\mathrm{e}0},\ i = 1,2.$$

For comparison with experimental data, it is often not the form of the distribution function that is of interest, but its integral characteristic. The concentration of ions is determined by the expression

$$n_i = \frac{n_{i0}}{1 + \Omega^2 t^2} N_i(\rho), \tag{7}$$

where

$$N_i = \exp\left(-\frac{\rho^2}{2V_{T_i}^2} - \frac{Z_i m}{M_i}\frac{\Phi}{V_{T_i}^2} \right)$$

is a universal function, which, as will be shown below, determines not only the distribution of particle concentration and flux, but also the asymptotic spectra of ions.

The flux of ions i, which is measured by sensors located at a distance r_0 in the radial direction from the axis, is found from the simple expression:

$$J_{r\,i}(t, r_0) = \frac{n_{i0}}{1 + \Omega^2 t^2} u_0 N_i(\rho_0), \tag{8}$$

where

$$\rho_0 = \frac{\Omega r_0}{\sqrt{1 + \Omega^2 t^2}};\ u_0 = \frac{\Omega^2 r_0 t}{1 + \Omega^2 t^2}.$$

The spectral distribution of accelerated ions in the radial direction with respect to energy is expressed as

$$\frac{\mathrm{d}N}{\mathrm{d}\epsilon_i} = \frac{2n_{0i}}{\Omega^2}\sqrt{\frac{\pi\chi}{\epsilon_i T_i}} \exp\left(-\frac{\chi\epsilon_i}{T_i} \right)$$
$$\times \int_0^\infty \mathrm{d}\rho\rho \cosh(b^i\rho) \exp\left(-\frac{Z_i m\Phi}{M_i V_{T_i}^2} - \frac{\rho^2\chi}{2V_{T_i}^2} \right), \tag{9}$$

where $\epsilon_i = (M_i/2)(v_r^i)^2$; $b^i = \Omega t\sqrt{2\epsilon_i\chi/T_i}/V_{T_i}$; and $\chi = 1 + \Omega^2 t^2$. Note that of particular interest are the spectra corresponding to the values observed in the experiment. Let us present an asymptotic expression, which can be obtained from (9) in the limit $\Omega t \to \infty$, using the saddle-point method:

$$\frac{dN_{\mathrm{as}}}{d\epsilon_i} = \frac{2\pi}{M_i\Omega^2} n_{i0} N_i\left(\rho = \sqrt{\frac{2\epsilon_i}{M_i}} \right). \tag{10}$$

Let us analyse the solution of the problem in a specific case, which is typical for the experiment, namely, when there are heavy ions (the main component, subscript '1') and lighter ions (impurity, '2'), i.e. $Z_2 M_1/(Z_1 M_2) > 1$ and $n_{20} < n_{10}$. Analysis of equation (6) allows an approximate solution to be obtained for the distribution of the plasma concentration and spectral distributions. In the equation for the potential (6), we select the dominant terms on the left- and right-hand sides. Equating them, we obtain approximate analytical expressions for the potential in the form of a binomial in ρ^2.

Let us first compare the terms on the left-hand side of (6), corresponding to hot and cold electrons. Then, we obtain the characteristic value of the potential

$$\Phi_{\mathrm{el}} = \rho^2/2 + V_{T_{\mathrm{c}}}^2 (1 - T_{\mathrm{c}}/T_{\mathrm{h}})^{-1} \ln(n_{\mathrm{h}0}/n_{\mathrm{c}0}). \tag{11}$$

It follows from the analysis of (6) that for $\Phi > \Phi_{\mathrm{el}}$ ($\Phi < 0$), the contribution of cold electrons dominates, and for $\Phi < \Phi_{\mathrm{el}}$ ($|\Phi| > |\Phi_{\mathrm{el}}|$) dominant is the contribution of hot electrons. Let

us now compare the contributions of ions of first and second types. Both contributions are compared at

$$\Phi_{\rm ion} = V_{T_{\rm c}}^2 \frac{T_1}{Z_1 T_{\rm c}}\left(\frac{Z_2 T_1}{Z_1 T_2} - 1\right)^{-1} \times\left[\ln\left(\frac{Z_2 n_{20}}{Z_1 n_{10}}\right) + \frac{\rho^2}{2V_{T_1}^2}\left(1 - \frac{T_1 M_2}{T_2 M_1}\right)\right]. \quad (12)$$

Note that when $\Phi > \Phi_{\rm ion}$, the contribution of ions of first type dominates, and for $\Phi < \Phi_{\rm ion}$ dominant is the contribution of ions of second type.

Thus, at small ρ, the main role in the equation for the potential is played by cold electrons and ions of main type. The balance of these contributions gives a decrease in the potential Φ (the growth of $|\Phi|$) to the largest of the two values, which is determined by expression (11) or (12), depending on the ratio of the problem parameters. A further decrease in the potential occurs according to one of two scenarios.

The first scenario (variant I) assumes a situation where the value of Φ falls to the value of $\Phi_{\rm ion}$ at $\rho = \rho_{\rm ion\,1}$. In the interval $0 < \rho < \rho_{\rm ion\,1}$, the potential is determined by the balance of cold electrons and the main ions. We give the corresponding expression, which is easily obtained from (6):

$$\Phi \approx \hat{\Phi}(\rho, Z_1, T_1, M_1, T_{\rm c}, n_{\rm c0}, n_{10}) = V_{T_{\rm c}}^2\left(1 + \frac{Z_1 T_{\rm c}}{T_1}\right)^{-1} \times\left[\frac{\rho^2}{2V_{T_1}^2}\left(\frac{T_1 m}{T_{\rm c} M_1} - 1\right) - \ln\left(\frac{n_{\rm c0}}{Z_1 n_{10}}\right)\right]. \quad (13)$$

In the interval $\rho_{\rm ion\,1} < \rho < \rho_{\rm el\,2}$, the potential distribution is determined by the balance of cold electrons and ions of second type (impurity ions). It can easily be obtained by replacing the subscript $1 \to 2$ in (13). The value of $\rho_{\rm el\,2}$ can be found from the solution of the equation $\Phi(\rho_{\rm el\,2}) = \Phi_{\rm el}(\rho_{\rm el\,2})$. In the region $\rho_{\rm el\,2} < \rho < \infty$, the approximate solution for the potential is determined by the balance of the hot electrons and ions of second type. This is obtained by replacing the subscripts c $\to$ h and $1 \to 2$.

The second possible scenario involves a decline in the potential from $\Phi(\rho = 0)$ to $\Phi_{\rm el}(\rho_{\rm el\,1})$ in the region $0 < \rho < \rho_{\rm el\,1}$, in which the distribution of Φ is determined by the balance of the cold electrons and the main ions (13); then, in the region $\rho_{\rm el\,1} < \rho < \rho_{\rm ion\,2}$ – by the balance of the hot electrons and the main ions; and finally, in the region $\rho_{\rm ion\,2} < \rho < \infty$ – by the balance of the hot electrons and ions of second type. Here, $\rho_{\rm el\,1}$ and $\rho_{\rm ion\,2}$ are found from the conditions $\Phi(\rho_{\rm el\,1}) = \Phi_{\rm el}(\rho_{\rm el\,1})$ and $\Phi(\rho_{\rm ion\,2}) = \Phi_{\rm ion}(\rho_{\rm ion\,2})$, where the functions $\Phi_{\rm el}$ and $\Phi_{\rm ion}$ are determined by expressions (11) and (12), and Φ – by the approximate solution (6), obtained as a result of the formal neglect by nondominant groups of particles [formula (13) and its analogues]. Thus, in the region dominated by hot electrons and lighter ions of second type ($Z_2/M_2 > Z_1/M_1$), we neglect the contribution of cold electrons and ions of first type.

Let us now consider the spectra of accelerated ions using the obtained approximate solutions. The analysis will be carried out for the first scenario. Expressions for the potential at finite times can be used to analytically describe the time evolution of the spectrum by calculating integral (9) with the help of the above representation of the potential in the form of a binomial. As a result, we obtain the expression in the form of a sum of three contributions:

$$\frac{{\rm d}N}{{\rm d}\epsilon_i} = \frac{2n_{0i}}{\Omega^2}\sqrt{\frac{\pi\chi}{T_i\epsilon_i}}\exp\left(-\frac{\chi\epsilon_i}{T_i}\right) \times(H(0,\rho_{\rm ion\,1}, a_1^i, b^i, c_1^i) + H(\rho_{\rm ion\,1},\rho_{\rm el\,2}, a_2^i, b^i, c_2^i) + H(\rho_{\rm el\,2},\infty, a_3^i, b^i, c_3^i)), \quad (14)$$

where

$$a_k^i = \frac{Z_i m_{\rm e}}{T_i}\varphi_{1k} + \frac{\chi}{2V_{T_i}^2};\ c_k^i = -\frac{Z_i m_{\rm e}}{T_i}\varphi_{0k};$$

the coefficients φ_{0k} and φ_{1k} are expressed in the following way: $\wedge\Phi_k = \varphi_{0k} + \rho^2\varphi_{1k}$; the function $\wedge\Phi_1$ is defined by expression (13); $\wedge\Phi_2 = \hat{\Phi}(\rho, Z_2, T_2, M_2, T_{\rm c}, n_{\rm c0}, n_{20})$; $\wedge\Phi_3 = \hat{\Phi}(\rho, Z_2, T_2, M_2, T_{\rm h}, n_{\rm h0}, n_{20})$; and the function

$$H(\rho_1,\rho_2,a',b',c') = \int_{\rho_1}^{\rho_2} {\rm d}\rho\,\rho\cosh(b'\rho)\exp(-a'\rho^2 + c')$$

is expressed in quadratures:

$$H = \frac{{\rm e}^{c'}}{8a'^{3/2}}\left\{-4\sqrt{a'}\,{\rm e}^{-a'\rho^2}\cosh(b'\rho) + \sqrt{\pi}\,b{\rm e}^{b'^2/4a'} \times\left[{\rm Erf}\left(\frac{2a'\rho - b'}{2\sqrt{a'}}\right) - {\rm Erf}\left(\frac{2a'\rho + b'}{2\sqrt{a'}}\right)\right]\right\}\Bigg|_{\rho_1}^{\rho_2}.$$

Here,

$${\rm Erf}(x) = \frac{2}{\sqrt{\pi}}\int_{-\infty}^{x}{\rm e}^{-\xi^2}{\rm d}\xi - 1$$

is the error function.

Let us consider in detail the spectral distributions in the limit $t \to \infty$. In this case, it is possible to obtain simple analytic formulas. In the region $\epsilon_\alpha < M_\alpha\rho_{\rm ion1}^2/2$, the energy spectra are written in the form:

$$\frac{{\rm d}N}{{\rm d}\epsilon_1} = \frac{2\pi}{M_1\Omega^2}n_{10}\left(\frac{n_{\rm c0}}{Z_1 n_{10}}\right)^{\left(1 + \frac{T_1}{Z_1 T_{\rm c}}\right)^{-1}} \times\exp\left[-\frac{\epsilon_1(1 + Z_1 m/M_1)}{Z_1 T_{\rm c} + T_1}\right],$$
$$\frac{{\rm d}N}{{\rm d}\epsilon_2} = \frac{2\pi}{M_2\Omega^2}n_{20}\left(\frac{n_{\rm c0}}{Z_1 n_{10}}\right)^{\left(\frac{Z_1 T_2}{Z_2 T_1} + \frac{T_2}{Z_2 T_{\rm c}}\right)^{-1}} \times\exp\left[-\frac{\epsilon_2(1 + Z_1 T_{\rm c}/T_1 - Z_2 T_{\rm c}/T_2 + Z_2 m T_1/M_1 T_2)}{Z_1 T_{\rm c}(T_2/T_1) + T_2}\right]. \quad (15)$$

In the interval $\rho_{\rm ion\,1} < \rho < \rho_{\rm el\,2}$ [corresponds to the interval $M_2(\rho_{\rm ion2})^2/2 < \epsilon < M_2(\rho_{\rm el2})^2/2$], we obtain

$$\frac{{\rm d}N}{{\rm d}\epsilon_2} = \frac{2\pi}{M_2\Omega^2}n_{20}\left(\frac{n_{\rm c0}}{Z_2 n_{20}}\right)^{\left(1 + \frac{T_2}{Z_2 T_{\rm c}}\right)^{-1}} \times \times\exp\left[-\frac{\epsilon_2(1 + Z_2 m/M_2)}{Z_2 T_{\rm c} + T_2}\right]. \quad (16)$$

In the interval $\rho_{el2} < \rho$ [corresponds to $\epsilon_2 > M_2(\rho_{el2})^2/2$], we have

$$\frac{dN}{d\epsilon_2} = \frac{2\pi}{M_2\Omega^2} n_{20}\left(\frac{n_{h0}}{Z_2 n_{20}}\right)^{\left(1+\frac{T_2}{Z_2 T_h}\right)^{-1}} \times \exp\left[-\frac{\epsilon_2(1+Z_2 m/M_2)}{Z_2 T_h + T_2}\right]. \quad (17)$$

Following the scheme described above, it is easy to derive formulas for the functions ρ^2_{ion1} and ρ^2_{el2}:

$$\rho^2_{ion1} = 2V_{T_1}^2\left[\left(\frac{Z_2 T_1}{Z_1 T_2} - 1\right)\left(1 - \frac{T_1 m}{T_c M_1}\right) + \left(1 - \frac{T_1 M_2}{T_2 M_1}\right)\left(1 + \frac{T_1}{Z_1 T_c}\right)\right]^{-1} \times\left[\left(\frac{Z_2 T_1}{Z_1 T_2} - 1\right)\ln\left(\frac{Z_1 n_1}{n_{c0}}\right) + \left(1 + \frac{T_1}{Z_1 T_c}\right)\ln\left(\frac{Z_1 n_{10}}{Z_2 n_{20}}\right)\right], \quad (18)$$

$$\rho^2_{el2} = 2V_{T_2}^2\left(1 + \frac{Z_2 m}{M_2}\right)^{-1}\left[\ln\left(\frac{Z_2 n_2}{n_{c0}}\right) - \left(\frac{1 + Z_2 T_c/T_2}{1 - T_c/T_h}\right)\ln\left(\frac{n_{h0}}{n_{c0}}\right)\right].$$

Below we present the results of a numerical solution of equation (6) and describe the integral characteristics. The obtained data are compared with the approximate expressions for spectra (15)–(18).

Let us now analyse the solution obtained. We choose the following parameters: $Z_1 = 3$, $M_1 = 15$, $Z_2 = 8$, $M_2 = 16$, $n_{20} = 10^{-3} n_{e0}$, $n_{h0}/n_{e0} = 3\times10^{-2}$, $T_h/T_c = 300$, $T_1/T_c = 10^{-2}$, and $T_2/T_1 = 1$.

Figure 1 shows the numerical solution of (6) for the potential. This solution is imposed on a piecewise smooth function (dashed curve) that is an approximate solution, the procedure for finding which is described above. Figures 1a and 1b correspond to different ranges of ρ^2 values. It follows from Fig. 1 that the proposed model agrees well with the found numerical solution (6). The distribution of the ion and electron concentrations is shown in Fig. 2. One can see the existence of characteristic regions, in which the charge balance is determined by cold electrons and a heavy ionic component, then by a light ionic impurity and cold electrons, and finally by hot electrons and impurity light ions at a greater distance from the axis of symmetry of the problem. The dynamics of the plasma can be traced by comparing Figs 2a and 2b. Note that at large times the flux becomes self-similar [27], and the concentration distribution and spectral distributions are determined by the universal function N_i [see formula (7)].

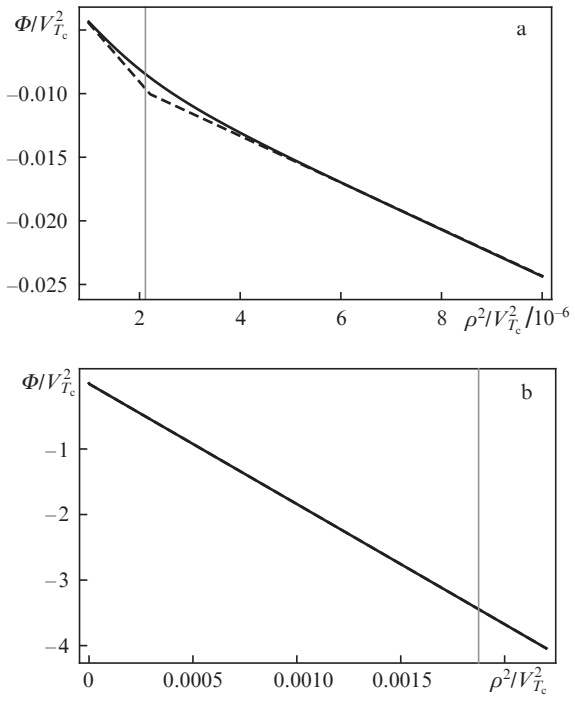

Figure 1. Dependence of the potential Φ on the variable ρ^2 (solid curve) and approximate dependence (dashed curve); (a) the range of small values of ρ^2, (b) the wider range of its values. Vertical gray lines indicate the values of (a) ρ^2_{ion1} and (b) ρ^2_{el2}.

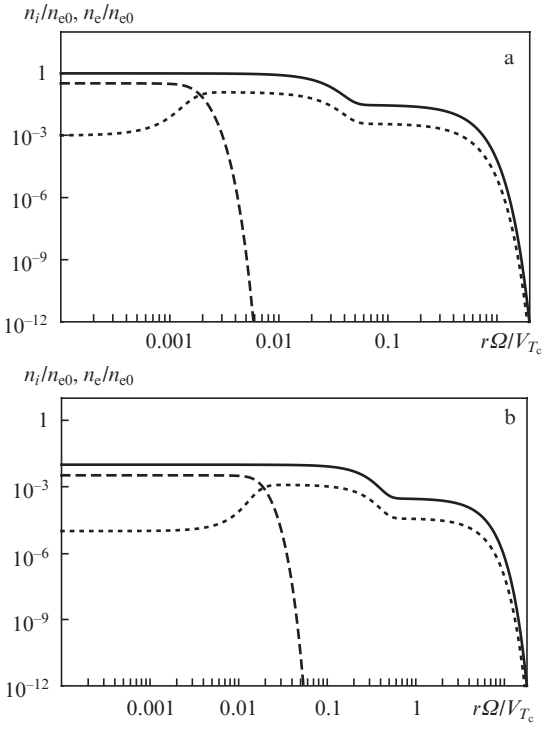

Figure 2. Spatial distributions of concentrations of the main (dashed curves) and impurity (dashed) ions. Solid curves correspond to the total electron concentration n_e. Distributions are presented for times (a) $t = 0$ and (b) $\Omega t = 10$.

The energy spectrum of impurity ions is shown in Fig. 3. The well-observed two slopes in the spectral distribution correspond to the transition from the region dominated by cold electrons to the region dominated by hot electrons, i.e., in accordance with formulas (11)–(15), at $\epsilon_2 \simeq M_2\rho^2_{el2}/2$.

Figure 4 shows the impurity ion current (8) observed at the detector. Two characteristic bursts are seen. First, fast ions (from the spatial region where the balance is determined by hot electrons) and then slow ions (from the region where the balance is determined by the cold electrons) contribute to the current. The time of arrival at the detector is determined by the sound velocity of the plasma; this means that the ions of main type will arrive at the detector much later. Their distribution in this case contains a single peak. In our opinion, of the two presented scenarios, the first one is the most typical, but in certain cases the second scenario can also be realised.

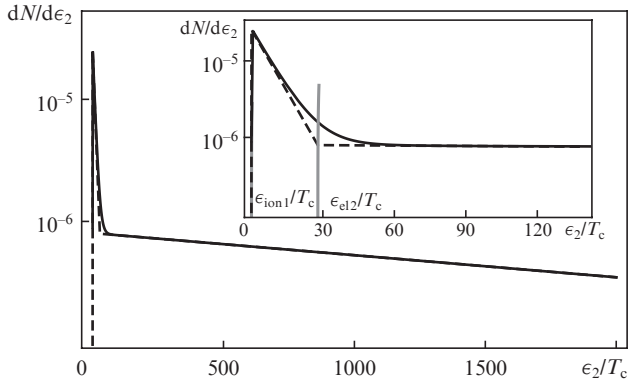

Figure 3. Asymptotic spectrum of light ions (solid curve) and approximation (dashed curve), obtained from formulas (15)–(18). The inset shows the range of low energies ($\epsilon < Z_2 T_h$), and the main figure – the entire range of interest. The gray lines indicate the quantities $\epsilon_{ion1} = M_2 \rho_{ion1}^2/2$ and $\epsilon_{el2} = M_2 \rho_{el2}^2/2$.

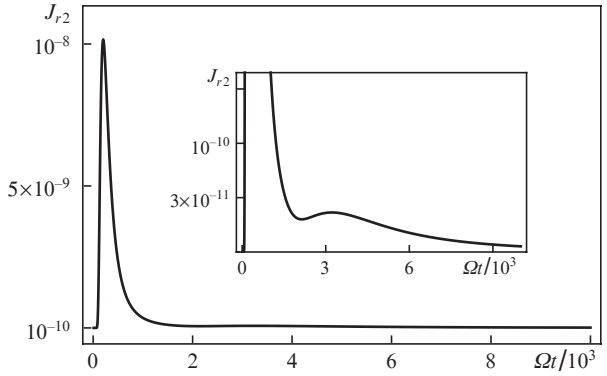

Figure 4. Normalised flux of impurity particles on the detector $[J_{r2}/(n_{e0} V_{T_c})]$, observed at a distance of $\Omega r/V_{T_c} = 100$. The inset shows a characteristic burst of the impurity ion current due to the presence of a two-temperature electron distribution.

4. Discussion of the results and conclusions

Using the group approach, we have derived in this paper a solution to a system of kinetic equations describing the dynamics of the radial expansion of a multicomponent plasma. The integral characteristics of ion acceleration are obtained, including the distribution of the densities and fluxes of particles (ions), as well as their energy spectra. The asymptotic solution found for the spectral function repeats the distribution of the ion concentration. Particular attention is paid to the analysis of the case, which is very typical for the experiment, when it is possible to select the main heavy component and a light low-density impurity. For this case, we obtain, in particular, simple asymptotic analytic expressions describing the spectral distributions of particles. A peculiar feature of the curves specifying the spectra of light ions is their proximity to a piecewise linear form and the presence of several slopes, which corresponds to the dominance of a particular group of particles. Thus, the developed model can be used to predict the characteristics of accelerated ions, for example, cylindrical nano-/microplasma or ion acceleration from the plasma channel.

Let us now compare the effectiveness of the considered thermal mechanism of ion acceleration with the ponderomotive mechanism of their acceleration by the example of a laser-heated cylindrical plasma channel [11, 29]. According to [29], the energy of laser-generated ions with ponderomotive acceleration is small in comparison with the energy accumulated during thermal expansion in the case of a sufficiently short laser pulse, i.e., when the condition

$$\tau_L < \frac{r_0}{c}\sqrt{\frac{M_{ion}}{Z_{ion}^2 m}\frac{\epsilon_{ion}}{mc^2}}\frac{(1+a_0^2)^{1/2}}{a_0^2}, \qquad (19)$$

is met, where r_0 is the radius of the channel and ϵ_{ion} is the characteristic energy of accelerated ions. For example, for the radiation parameters of a Ti : sapphire laser with a wavelength $\lambda = 0.8$ μm, intensity $I_L \simeq 5\times10^{18}$ W cm^{-2}, which corresponds to a dimensionless field amplitude $a_0 \approx 1.5$ ($a_0 = 0.85\times 10^{-9}\lambda$ [μm] $I_L^{1/2}$ [W cm^{-1}]^2), pulse duration $\tau_L \approx 30$ fs and the channel radius $r_0 = 4$ μm, we find that in the case of acceleration of protons, the ratio of the energy acquired by them from the ponderomotive mechanism to the characteristic energy for protons under thermal expansion ($\epsilon_2 \simeq T_h$) is $\sim10^{-2}$. We assume here that the temperature of the hot electron component is determined by the commonly used ponderomotive scaling: $T_h \simeq mc^2(\sqrt{1+a_0^2}-1) \approx 400$ keV [30].

As noted in the Introduction, new innovative laser targets are targets of 'nano-forest' type [13, 14]. In our opinion, these targets, for example, a target made of titanium nano-/microwires with the addition of deuterium, are promising for triggering nuclear DT reactions and generating neutrons. Indeed, the high average density of such a coating can provide a high yield of neutrons. It is known that a DT-reaction efficiently occurs at a relatively low energy of colliding particles ($\sim$100 keV); therefore, unlike the problem of laser generation of high-energy ions, ultra-high densities of the energy flux of laser radiation are not required. If we consider a laser-heated target surface in the form of cylindrical TiD wires of diameter $D \sim 150$ nm and an average separation of $\sim$500 nm between them, then such a characteristic energy (100 keV) will be acquired by deuterons at a laser radiation intensity $I_L \simeq 10^{18}$ W cm^{-2} during the expansion time of the wire to a distance of the order of the characteristic distance between the wires.

The estimates obtained above are based on the assumption of a quasi-neutral character of the plasma expansion. However, under irradiation of nanotargets, a transition from a quasi-neutral regime to a regime with a strong charge separation and, in the limit, to the Coulomb explosion regime, is possible. This occurs for $\lambda_D/D > 1$ [$\lambda_D = \sqrt{T_e/(4\pi n_{e0} e^2)}$ is the Debye radius and D is the diameter of the nanocylinder]. For the above example, $\lambda_D/D \approx 5\times10^{-2}$ for $n_{e0} \approx 5\times10^{23}$ cm^{-3} and, therefore, $\lambda_D \approx 7$ nm, i.e., the expansion regime is close to quasi-neutral. Thus, the expansion will occur in the quasi-neutral or close-to-quasi-neutral regime, if only not very thin ($D \lesssim 10$ nm) wires are used.

In conclusion, we note the prospects of using high-power short-wavelength (ultraviolet) lasers (see, for example, [31]). The transition to short-wavelength radiation will further increase the effective density of the nanostructured target surface and, consequently, the yield of neutrons, due to the convergence of deuterium-enriched nano-/microwires, without reducing the penetration depth of laser radiation. A more detailed study of a neutron source based on targets of this type will be carried out elsewhere.

Acknowledgements. The work was supported by the Russian Science Foundation (Grant No. 17-12-01283).

Appendix. The Lie group of point transformations

The Lie group of point continuous transformations (admissible by the system of kinetic equations for the velocity of the distribution functions of particles of type α, integrated with respect to the z-component, i.e., for $f_{\perp}^{\alpha}$, and by the nonlocal quasi-neutrality condition) has the most visible form in rectangular coordinates. Considering the transformations in the plane perpendicular to the z axis, we write the corresponding infinitesimal operators of the point symmetry group (for details of the calculation of the symmetries for systems of integrodifferential equations, see [32]):

$$X_0 = \frac{\partial}{\partial t},\ \ X_1 = \frac{\partial}{\partial x},\ \ X_2 = \frac{\partial}{\partial y},\ \ Y_1 = \sum_{\alpha} f^{\alpha}\frac{\partial}{\partial f^{\alpha}},$$

$$Y_2 = x\frac{\partial}{\partial x} + y\frac{\partial}{\partial y} + \sum_{\alpha}\left(v_x^{\alpha}\frac{\partial}{\partial v_x^{\alpha}} + v_y^{\alpha}\frac{\partial}{\partial v_y^{\alpha}}\right) + E_x\frac{\partial}{\partial E_x} + E_y\frac{\partial}{\partial E_y},$$

$$Y_3 = 2t\frac{\partial}{\partial t} + x\frac{\partial}{\partial x} + y\frac{\partial}{\partial y} - \sum_{\alpha}\left(v_x^{\alpha}\frac{\partial}{\partial v_x^{\alpha}} + v_y^{\alpha}\frac{\partial}{\partial v_y^{\alpha}}\right) - 3E_x\frac{\partial}{\partial E_x} - 3E_y\frac{\partial}{\partial E_y}, \qquad \text{(A1)}$$

$$G_1 = t\frac{\partial}{\partial x} + \sum_{\alpha}\frac{\partial}{\partial v_x^{\alpha}},\ \ G_2 = t\frac{\partial}{\partial y} + \sum_{\alpha}\frac{\partial}{\partial v_y^{\alpha}},$$

$$Z = y\frac{\partial}{\partial x} - x\frac{\partial}{\partial y} + \sum_{\alpha}\left(v_y^{\alpha}\frac{\partial}{\partial v_x^{\alpha}} - v_x^{\alpha}\frac{\partial}{\partial v_x^{\alpha}}\right) + E_y\frac{\partial}{\partial E_x} - E_x\frac{\partial}{\partial E_y},$$

$$X_{\mathrm{pr}} = t^2\frac{\partial}{\partial t} + tx\frac{\partial}{\partial x} + ty\frac{\partial}{\partial y} + \sum_{\alpha}\left[(x - v_x^{\alpha}t)\frac{\partial}{\partial v_x^{\alpha}} + (y - v_y^{\alpha}t)\frac{\partial}{\partial v_y^{\alpha}}\right] - 3tE_x\frac{\partial}{\partial E_x} - 3tE_y\frac{\partial}{\partial E_y}.$$

Operators (A1) have a simple physical meaning: the first three operators, X_0, X_1 and X_2, correspond to the time transfer transformations t and the coordinates x and y. The following three operators, Y_1, Y_2 and Y_3, describe the transformation of stretching. The transformations with the operators G_1 and G_2 correspond to Galilean transformations along the x and y axes, respectively, and the operator Z corresponds to the rotation transformation in the $\{x, y\}$ plane. Finally, the operator X_{pr} corresponds to the group of projective transformations.

The axially symmetric invariant-group solution arises in using the two-dimensional algebra $L_2 = \{Z, R\}$ composed of the rotation operator Z and the operator $R = X_0 + \Omega^2 X_{\mathrm{pr}}$ and represents a linear combination of the time shift operator X_0 and the projective group operator X_{pr}. In cylindrical geometry, the operator $Z = \partial/\partial\varphi$ corresponds to a shift in angle φ, and the operator R is expressed as:

$$R = (1 + \Omega^2 t^2)\frac{\partial}{\partial t} + \Omega^2 tr\frac{\partial}{\partial r} + \Omega^2 + \Omega^2\sum_{\alpha}\left[(r - tv_r^{\alpha})\frac{\partial}{\partial v_r^{\alpha}} - tv_{\varphi}^{\alpha}\frac{\partial}{\partial v_{\varphi}^{\alpha}}\right] - 3\Omega^2 tE_r\frac{\partial}{\partial E_r} - 3\Omega^2 tE_{\varphi}\frac{\partial}{\partial E_{\varphi}}. \qquad \text{(A2)}$$

Invariance with respect to the operator Z gives an axially symmetric solution that does not depend on the angular variable φ, and the renormalisation-symmetry operator R specifies finite transformations relating the initial values of the particle distribution functions and the electric field at $t = 0$ with their values for $t \neq 0$, i.e., it gives the required solution of the initial problem for equations (1), (2) with initial conditions corresponding to the isotropic initial Maxwellian distribution functions of particles with homogeneous initial temperature and zero initial mean velocity. In this case, the solution is expressed in terms of the invariants of the operator R,

$$i_0 = \frac{r}{\sqrt{1 + \Omega^2 t^2}},\ i_{\alpha 1} = \sqrt{1 + \Omega^2 t^2}\,v_r^{\alpha} - \frac{\Omega^2 tr}{\sqrt{1 + \Omega^2 t^2}},$$

$$i_{\alpha 2} = \sqrt{1 + \Omega^2 t^2}\,v_{\varphi}^{\alpha},\ i_{\alpha 3} = f_{\perp}^{\alpha},\ i_4 = E_r(1 + \Omega^2 t^2)^{3/2}, \qquad \text{(A3)}$$

$$i_5 = E_{\varphi}(1 + \Omega^2 t^2)^{3/2}.$$

For the solution considered in the paper with $E_{\varphi} = 0$, the invariant i_5 is zero, and the relation between $i_{\alpha 3}$ and i_4 with the remaining invariants is given by formulas (3), (4).

References

1. Bychenkov V.Yu., Tikhonchuk V.T., Tolokonnikov S.V. *JETP*, **88** (6), 1137 (1999) [*Zh. Eksp. Teor. Fiz.*, **115** (6), 2080 (1999)].
2. Bulanov S.V., Khoroshkov V.S. *Plasma Phys. Rep.*, **28**, 453 (2002) [*Fiz. Plazmy*, **28**, 493 (2002)].
3. Nemoto K., Maksimchuk A., Banerjee S., et al. *Appl. Phys. Lett.*, **78**, 595 (2001).
4. Bychenkov V.Yu., Brantov A.V., Mourou G. *Laser Part. Beams*, **32**, 605 (2014).
5. Borghesi M. et al. *Plasma Phys. Control. Fusion*, **43**, A267 (2001).
6. Mackinnon A.J. et al. *Rev. Sci. Instrum.*, **75**, 3531 (2004).
7. Roth M. et al. *Phys. Rev. Lett.*, **86**, 436 (2001).
8. Bychenkov V.Yu., Rozmus W., Maksimchuk A., et al. *Plasma Phys. Rep.*, **27**, 1017 (2001) [*Fiz. Plazmy*, **27**, 1076 (2001)].
9. Daido H., Nishiuchi M., Pirozhkov A.S. *Rep. Progr. Phys.*, **75**, 056401 (2012).
10. Bychenkov V.Yu., Brantov A.V., Govras E.A., Kovalev V.F. *Phys. Usp.*, **58**, 71 (2015) [*Usp. Fiz. Nauk*, **185**, 77 (2015)].
11. Sarkisov G.S., Bychenkov V.Y., Novikov V.N., et al. *Phys. Rev. E*, **59**, 7042 (1999).
12. Murakami M., Tanaka M. *Appl. Phys. Lett.*, **102**, 163101 (2013).
13. Lećz Zs., Andreev A. *Phys. Plasmas*, **24**, 033113 (2017).
14. Bargsten C., Hollinger R., Capeluto M.G., et al. *Sci. Adv.*, **3**, e1601558 (2017).
15. Gurevich A.V., Pariiskaya L.V., Pitaevskii L.P. *Sov. Phys. JETP*, **22**, 449 (1966) [*Zh. Eksp. Teor. Fiz.*, **49**, 647 (1965)].
16. Nishihara K., Amitani H., Murakami M., et al. *Nucl. Instrum. Methods Phys. Res. A*, **464**, 98 (2001).
17. Kovalev V.F., Bychenkov V.Yu. *JETP*, **101** (2), 212 (2005) [*Zh. Eksp. Teor. Fiz.*, **128** (2), 243 (2005)].
18. Popov K.I., Bychenkov V.Yu., Rozmus W., et al. *Laser Part. Beams*, **27**, 321 (2009).
19. Dorozhkina D.S., Semenov V.E. *JETP Lett.*, **67**, 573 (1998) [*Pis'ma Zh. Eksp. Teor. Fiz.*, **67**, 543 (1998)].
20. Kovalev V.F., Bychenkov V.Yu., Tikhonchuk V.T. *JETP*, **95**, 226 (2002) [*Zh. Eksp. Teor. Fiz.*, **122**, 264 (2002)].
21. Mora P. *Phys. Rev. Lett.*, **90**, 185002 (2003).
22. Bochkarev S.G., Bychenkov V.Yu., Tikhonchuk V.T. *Plasma Phys. Rep.*, **32** (3), 205 (2006) [*Fiz. Plazmy*, **32** (3), 230 (2006)].
23. Bochkarev S.G., Golovin G.V., Uryupina D.S., Shulyapov S.A., Andriyash A.V., Bychenkov V.Yu., Savel'ev A.B. *Phys. Plasmas*, **19**, 103101 (2012).
24. Govras E.A., Bychenkov V.Yu. *JETP Lett.*, **98**, 70 (2013) [*Pis'ma Zh. Eksp. Teor. Fiz.*, **98**, 78 (2013)].

25. Kahaly S., Sylla F., Lifschitz A., et al. *Scientific Rep*., **6**, 31647 (2016).
26. Lifschitz A., Sylla F., Kahaly S., et al. *New J. Phys*., **16**, 033031 (2014).
27. Kovalev V.F., Bychenkov V.Yu., Tikhonchuk V.T. *JETP Lett*., **74**, 10 (2001) [*Pis'ma Zh. Eksp. Teor. Fiz*., **74**, 12 (2001)].
28. Kovalev V.F., Bychenkov V.Yu. *Phys. Rev. Lett*., **90** (18), 185004 (2003).
29. Sarkisov G.S., Bychenkov V.Yu., Novikov V.N., et al. *Phys. Rev. E*, **59** (6), 7042 (1999).
30. Wilks S.C., Kruer W.L., Tabak M., Langdon A.B. *Phys. Rev. Lett*., **69**, 1383 (1992); Malka G., Miquel J.L. *Phys. Rev. Lett.*, **77**, 75 (1996).
31. Zvorykin V.D., Didenko N.V., Ionin A.A., et al. *Laser Part. Beams*, **25**, 435 (2007).
32. Grigoriev Y.N., Ibragimov N.H., Kovalev V.F., Meleshko S.V. *Lecture Notes in Physics* (Heidelberg: Springer, 2010) Vol. 806.